Ligand-field splitting of Fe^{2+} in distorted octahedral sites of the magnesium-rich orthopyroxenes $Fe_xMg_{1-x}SiO_3$: Correlation of magnetic susceptibility, Mössbauer, and optical absorption spectra

G. Y. V. Victor,[1] Debjani Ghosh,[1] and Subrata Ghose[2]
[1]*Solid State Physics Department, Indian Association for the Cultivation of Science, Jadavpur, Calcutta 700 032, India*
[2]*Mineral Physics Group, Department of Earth and Space Sciences, Box 351310, University of Washington, Seattle, Washington 98195*
(Received 24 January 2001; revised manuscript received 20 May 2001; published 19 September 2001)

Orthopyroxenes, $Fe_xMg_{1-x}SiO_3$, ranging in composition between the Fe and Mg end members, represent an interesting system from the physical point of view because of the strong site preference of Fe^{2+} for one of the two octahedral sites in the crystal structure. For Mg-rich samples with $x<0.5$, a major portion of the Fe^{2+} ions reside in the distorted octahedral $M2$ site and the magnetic susceptibility and optical absorption spectra are dominated by the effects of Fe^{2+} in this site. Two natural orthopyroxenes with $x=0.12$ and 0.20 have been investigated by magnetic susceptibility measurements and Mössbauer spectroscopy. The thermal characteristics of the observed mean magnetic susceptibility $\overline{\chi}$ and the quadrupole splitting ΔE_Q were analyzed using ligand-field theory. A minimum number of approximations were made to modify the Hamiltonian for Fe^{2+} in the distorted octahedral $M2$ site. The electronic energy-level pattern and the corresponding wave functions were obtained from a best fitting of the experimental results with the corresponding theoretical values. These results were used to calculate the thermal characteristics of the crystalline magnetic susceptibilities χ_a, χ_b, and χ_c, arising from Fe^{2+} in the $M1$ and $M2$ sites in the ratio of their occupancies. The directional magnetic susceptibilities $\chi_b>\chi_c>\chi_a$ are in agreement with the corresponding values in orthopyroxenes with higher concentration of Fe^{2+}. The energy-level diagram of Fe^{2+} at the $M2$ site agrees well with the optical absorption spectra resulting mainly from Fe^{2+} at the $M2$ site. There is very little variation in ΔE_Q for Fe^{2+} at the $M2$ site as a function of temperature compared with that in the regular octahedral $M1$ site which shows a large variation. The ΔE_Q of Fe^{2+} at the $M2$ site and the magnetic susceptibility show very little variation with chemical composition. Our analysis also suggests considerable overlap of the molecular orbitals of the ligand electrons with those of the Fe^{2+} ions.

DOI: 10.1103/PhysRevB.64.144413 PACS number(s): 75.50.Bb, 76.80.+y

I. INTRODUCTION

Orthopyroxenes, $Fe_xMg_{1-x}SiO_3$, are important rock-forming ferromagnesian silicates representing a complete solid solution between the Mg end member ($MgSiO_3$, enstatite, En) and the iron end member ($FeSiO_3$, ferrosilite, Fs). Because of the very strong site preference of the Fe^{2+} ion for one of the two octahedral sites in the crystal structure, orthopyroxenes (OPX) represent an interesting system from the physical point of view. For Mg-rich samples with $x<0.5$, a major portion of the Fe^{2+} ions reside in the distorted octahedral $M2$ site and the magnetic susceptibility and the optical absorption spectra are dominated by the effects of the Fe^{2+} ions in this site. Only for Fe-rich compositions with $x>0.5$ do the effects of the Fe^{2+} ions in the regular octahedral site $M1$ begin to be discernible. In the present paper, we report the results of Mössbauer spectroscopy (MS) experiments and magnetic susceptibility measurements on two natural magnesium-rich orthopyroxene samples with $x=0.12$ (En_{88}) and 0.20 (En_{80}), known as enstatites. Mössbauer spectroscopy has been widely used for the determination of the site occupancies of Fe^{2+} and Mg^{2+} ions in different crystallographic sites and Mg^{2+}-Fe^{2+} order-disorder in ferromagnesian silicates.[1–6] Although measurements of MS (Refs. 2–5 and 7–9) and magnetic susceptibilities of OPX with higher concentrations of Fe^{2+} have been reported,[9,10] there are no previous reports of magnetic and MS studies on enstatites with low Fe^{2+} concentrations. Crystallographic structure determinations and optical absorption spectra in the infrared and visible regions of enstatites with lower values of x have been reported.[11–14] These results can be used to analyze our magnetic and MS results as well as the optical absorption spectra within the context of the ligand-field (LF) theory using a minimum number of approximations.

In orthopyroxenes, Fe^{2+} exists as the high-spin species.[2] The crystal structure of orthopyroxene (orthorhombic, space group *Pbca*) consists of single silicate chains $(SiO_3)_\infty$, held together by divalent Fe and Mg cations in octahedral coordination with six oxygen ligands from the silicate groups.[15,16] There are two nonequivalent crystallographic octahedral sites $M1$ and $M2$. The $M2$ site is more distorted due to the fact that each of the two ligand oxygens is shared with two silicon atoms resulting in longer M-O distances compared to the other four oxygen atoms bonded to one silicon atom each[15–17] [Fig. 1(a)]. $M1$ lies in the interior of the double octahedral band and $M2$ lies exterior to it, giving rise to a zigzag pattern of the Fe^{2+}, Mg^{2+} cation arrangement in the structure[18] [Figs. 1(b) and 1(c)]. It has been known that in a crystal structure, when the octahedral sites are distorted to different degrees from octahedral symmetry, Fe^{2+} ions exhibit a tendency to enrich in the more distorted site.[16,19,20] In the case of orthopyroxenes, Fe^{2+} enrichment takes place at the $M2$ site as evidenced from earlier single-crystal x-ray diffraction[16] and MS studies[2–5,7–9] as well as from studies of

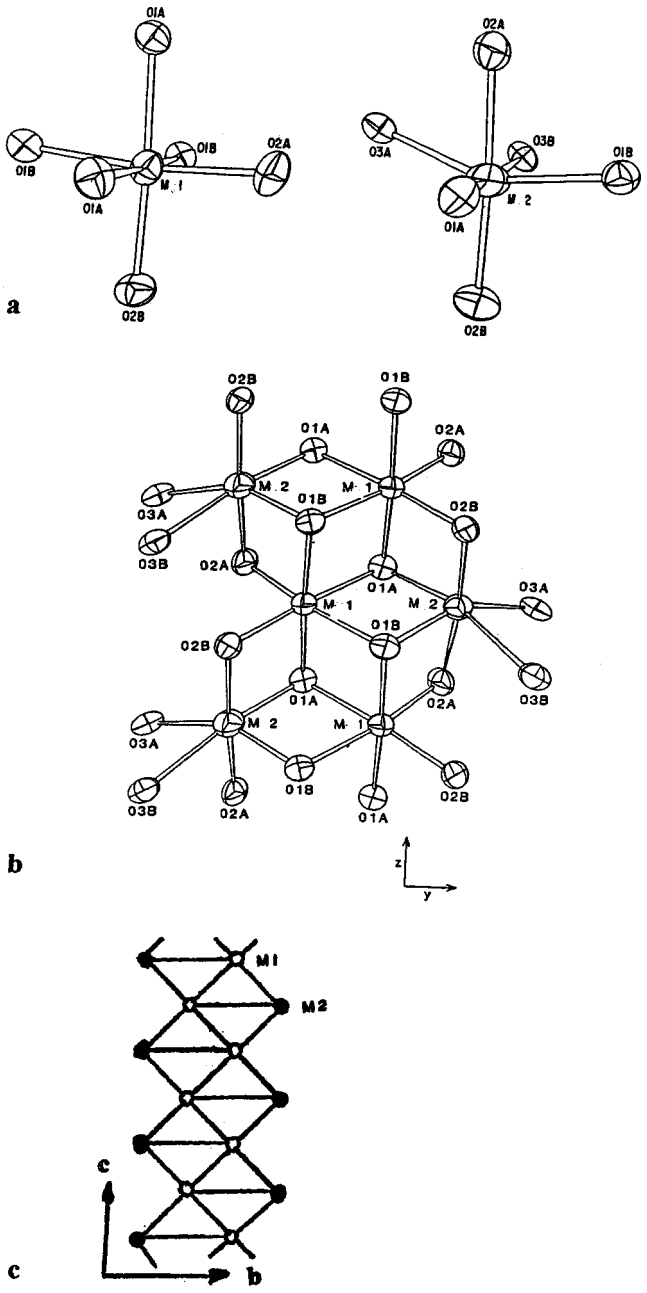

FIG. 1. Crystallographic structure of orthopyroxene (OPX). (a) Configuration of the $M1$ and $M2$ octahedra. (b) The double-octahedral band formed by edge sharing $M1$ and $M2$ octahedra. (c) Arrangement of the Fe^{2+} and Mg^{2+} cations in orthopyroxene. Open circles: $M1$ site. Solid circles: $M2$ site.

optical absorption spectra[11–14] and neutron diffraction.[9] The dependence of the occupancy of Fe^{2+} at $M1$ and $M2$ sites with different values of x are shown by the two curves in Fig. 2, the data points of which have been collected from a survey of earlier studies.[2,3,5,7–9] Since the occupancy factors of Fe^{2+} atoms at $M1$ and $M2$ sites for $x<0.25$ have been reported for very few samples, we wanted to find out whether the occupancy factors determined from chemical analysis and MS studies of the two samples, En_{88} and En_{80} with $x=0.12$ and $x=0.20$, respectively, follow the same curves for $M1$ and $M2$ site occupancies shown in Fig. 2. We also

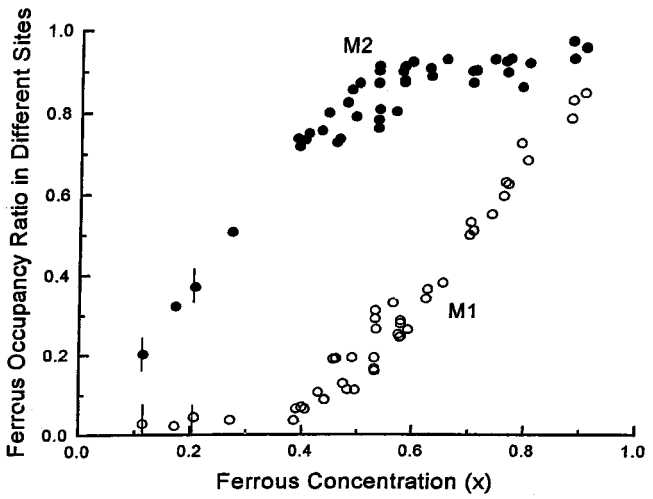

FIG. 2. Occupancy of Fe^{2+} at $M1$ and $M2$ sites in OPX with different concentrations of x (occupancy ratios of En_{88} and En_{80} in $M1$ and $M2$ sites are indicated by ϕ and ●).

wished to determine the dependence of different thermophysical properties on the occupancy of Fe^{2+} at the two different sites in OPX samples with different values of x by investigating the near end members, i.e., magnesium-rich and iron-rich OPX samples.[9,10] The results of our investigations on the iron-rich samples of OPX will be reported in a separate paper.

Earlier workers[11–14] studied the optical spectra of a bronzite, En_{85}, and a hypersthene, $Fs_{39.5}$, observing bands around 11 000, 5400, and 3100 cm^{-1} in the α, β, and γ spectra taken along the b, a, and c axes of the crystal, respectively. These bands were assigned to different transitions between the energy levels arising from the ground term ^5D of the $3d^6$ configuration of the Fe^{2+} ion placed at the noncentrosymmetric distorted $M2$ site, which is subjected to different perturbations like spin-orbit coupling and considerable distortion from the regular octahedral symmetry. The spectra from Fe^{2+} at the $M1$ site was not observed as it was much weaker and may have been overlapped by the stronger absorption lines due to the former. Later, Goldman and Rossman[14] studied the spectra of a bronzite, En_{85}, and found a band at 2350 cm^{-1} instead of 3100 cm^{-1} as reported earlier.[11,13] They also analyzed the spectra of Fe^{2+} at the $M2$ site considering C_{2v} symmetry using the crystal-field (CF) theory based on a point charge model appropriate for an ionic system and neglected the spin-orbit interaction as well as the covalency effect. In contrast, we have applied the more relevant LF theory, since it is well known[21–23] that LF levels of Fe^{2+} ions can be determined from a fitting of the thermal characteristics of the quadrupole splitting measured from the Mössbauer spectra and magnetic susceptibility results that can be cross-checked with the available optical absorption spectra.

II. EXPERIMENTAL RESULTS

A. Chemical analysis of the samples

Enstatites, En_{88} and En_{80} with $x=0.12$ and 0.20, were separated from a chromite pyroxenite from the

TABLE I. Mössbauer parameters for enstatites (En_{88} and En_{80}). ΔE_Q: quadrupole spliting. δ: isomer shift. Γ: linewidth. OF: fractional intensity. Fe^{2+}-OF: Fe^{2+} occupancy factor.

Temperature (K)	ΔE_Q (mm/s)	δ (mm/s)	Γ (mm/s)	OF (%)	Fe^{2+} (OF)	ΔE_Q (mm/s)	δ (mm/s)	Γ (mm/s)	OF (%)	Fe^{2+} (OF)
En_{88}			M1					M2		
300	2.091	1.237	0.3304	12.0	0.028	1.853	1.112	0.228	88.0	0.2026
80	2.601	1.273	0.4562	12.0	0.028	2.004	1.138	0.261	88.0	0.2026
En_{80}			M1					M2		
300	2.212	1.201	0.3234	10.6	0.044	1.871	1.141	0.3017	89.4	0.3698
80	2.90	1.252	0.4503	10.6	0.044	2.027	1.177	0.3453	89.4	0.3698

Kondapalli region (16° 37′ N, 80° 32′ E) in Eastern Ghats, Andhra Pradesh, India. Powder x-ray diffraction lines confirmed that the samples belong to the enstatite region with compositions, En_{80} and En_{88}, and are free of any inclusions of augite or diopside that also contain Fe^{2+}. Rao[24] reported that the orthopyroxenes from this region have compositions rich in enstatite with En between 78 and 90. From wet chemical analyses, the chemical compositions for the samples En_{80} and En_{88} were found as follows:

sample I(En_{80}): $(Ca_{0.0152}Mn_{0.0064}Mg_{0.7502}Fe_{0.1956}{}^{2+}Ti_{0.01}Al_{0.0226})_{1.0}(Si_{0.9577}Al_{0.0423})_{1.0}O_3$,

sample II(En_{88}): $(Ca_{0.0072}Mn_{0.0015}Mg_{0.8698}Fe_{0.1131}{}^{2+}Ti_{0.0016}Al_{0.0068})_{1.0}(Si_{0.9624}Al_{0.0376})_{1.0}O_3$.

B. Mössbauer experiment

Mössbauer experiments were carried out on a conventional spectrometer with a constant-velocity drive (Wissel 1000 model) and a cold-finger-type liquid-nitrogen cryostat for measurements down to 80 K. ^{57}Co in a Rh matrix was used as the radiation source, and the isomer shift refers to the symmetry shift of the six-line magnetic pattern from the α-Fe foil. The data were collected in 512 channels. The average counts recorded at room and low temperatures were ~ 8 and $\sim 3\times 10^5$, respectively.

Enstatites exhibit two overlapping quadrupole-split doublets with asymmetric peaks from ferrous-ionic states at the $M1$ and $M2$ sites. The spectra were analyzed and fitted by a least-squares program[25] without constraints. The quadrupole splitting ΔE_Q, isomer shifts δ, linewidth Γ, and the intensity ratios for the two samples are shown in Table I.

On cooling the sample, quadrupole splitting ΔE_Q of Fe^{2+} in $M1$ increased by 24.4% and 31.1%, whereas for Fe^{2+} in the $M2$ site, ΔE_Q increased by 9.5% and 9.6% for En_{88} and En_{80}, respectively. The stronger temperature variation of ΔE_Q for Fe^{2+} in the $M1$ site reflects a small separation of the lowest crystalline field states and the weak temperature dependence of that in the $M2$ site is an indication of unusually large separation of the $^5T_{2g}$ level as also noted by others.[7–9] ΔE_Q vs T curves obtained for Fe^{2+} at both the sites for the two enstatite samples are shown in Fig. 3 along with those reported earlier[8,9] for samples with different values of x; the inset shows the ΔE_Q values at 77 K for samples with different values of x.

The linewidths from Fe^{2+} in $M1$ and $M2$ on cooling increase by 39.2% and 14.6% for En_{80} and 38.2% and 14.4% for En_{88}, which is an indication for relaxation effects found generally in dilute silicate minerals with $x<0.4$.[7,8] The differences in the isomer shifts for Fe^{2+} in the two crystallographic sites of En_{88} and En_{80} indicate covalency effect.[26] The smaller isomer shift for Fe^{2+} in the $M2$ site suggests a comparatively higher degree of covalency. From isomer shift, Ingalls[21] reported the covalency factor for $FeSiF_6\ 6H_2O$

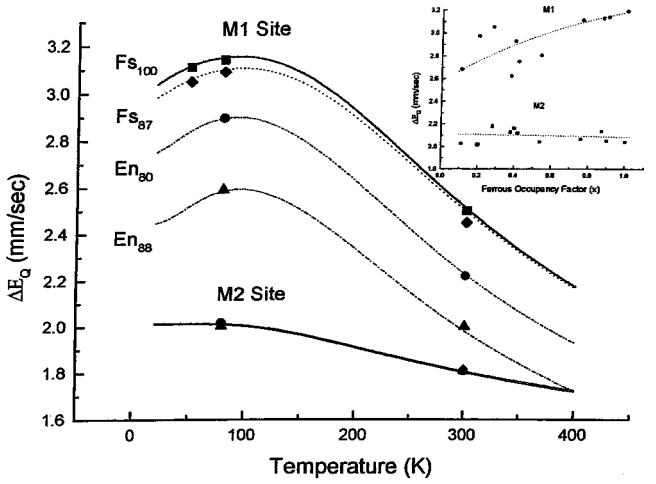

FIG. 3. The thermal characteristics (experimental points and theoretical curves) of ΔE_Q vs T curves for En_{88}, En_{80}, Fs_{87}, and Fs_{100} and the inset shows the ΔE_Q values of different compositions of x.

to be 0.85 and Tofield[26] established that the *d* electrons are delocalized in silicate minerals. The fact that the iron end member, ferrosilite ($FeSiO_3$), undergoes a paramagnetic to antiferromagnetic transition at 40 K is also an indication of considerable *d*-electron delocalization because of the long superexchange path involved [Fe^{2+}-O-Si-O-Fe (Ref. 2)] between two octahedral bands of Fe^{2+} (the spins of which are antiferromagnetically ordered) separated by the silicate chains.[10]

Analysis of the Mössbauer spectra of En_{80} and En_{88} indicates that Fe^{2+} is enriched in the $M2$ site in the ratio of 8.4:1 and 7.3:1 compared with the $M1$ site. The intensity ratio between the quadrupole-split doublets from Fe^{2+} in $M1$ and $M2$ is 1:8, $M2$ having greater intensity.[2,8,9] The occupancy factors for Fe^{2+} in different crystallographic sites are the products of the fractional intensity observed from MS and the total atomic ratio $2Fe^{2+}/(Fe^{2+}+Mg)$ obtained from the chemical analysis.[3,5] The site occupancy factors and the actual chemical compositions for the enstatites determined by standard method[3,5] are as follows:

sample I [$En_{80}(Mg_{0.80}Fe_{0.20}SiO_3)$]: 4.5% Fe^{2+} and 95.5% Mg^{2+} in M_1 site; 36.8% Fe^{2+} and 63.2% Mg^{2+} in M_2 site,

sample II [$En_{88}(Mg_{0.88}Fe_{0.12}SiO_3)$]: 3% Fe^{2+} and 97% Mg^{2+} at M_1 site; 20% Fe^{2+} and 80% Mg^{2+} at M_2 site.

The actual chemical compositions of the two samples are

$$\text{sample I}(En_{80}):\quad (Mn_{0.01}Ca_{0.03}Fe_{0.35}{}^{2+}Mg_{0.61})_{1.0}(Al_{0.05}Ti_{0.02}Fe_{0.04}{}^{2+}Mg_{0.89})_{1.0}(Si_{1.92}Al_{0.08})_{2.0}O_6,$$

$$\text{sample II}(En_{88}):\quad (Mn_{0.01}Ca_{0.01}Fe_{0.20}{}^{2+}Mg_{0.78})_{1.0}(Al_{0.01}Ti_{0.0}Fe_{0.03}{}^{2+}Mg_{0.95})_{1.0}(Si_{1.92}Al_{0.08})_{2.0}O_6.$$

The occupancy factors for En_{88} and En_{80} are shown in Fig. 2. Inspection shows that these points lie on the curve drawn through the points for higher values of *x* and the origin.

C. Magnetic susceptibility measurements

Magnetic susceptibilities of the polycrystalline natural samples were measured between 400 and 77 K in an electrodynamically controlled Curie-type balance using the Faraday method. The susceptibility increased by about 453% for En_{80} and 452% for En_{88}, respectively, at the lowest temperature. The Curie temperatures θ_p were found to be 36.5 and 35.8 K, and the corresponding Curie constants C_m were 3.13 and 3.18 for En_{88} and En_{80}, respectively. The average effective magnetic moments at 400 and 80 K are 5.57 μ_β, 5.31 μ_β and 5.53 μ_β, 5.26 μ_β for En_{80} and En_{88}, respectively. A sharp increase of the susceptibility values below 200 K indicated large orbital contributions, as also observed[9,10] for higher concentration of ferrous iron with $x>0.8(Fs_{87})$.

III. THEORY

When the free-ion $3d^6$ state of Fe^{2+} is acted upon by a LF with octahedral (O_h) symmetry, the fivefold degeneracy of the ^5D state is lifted, resulting in a $^5T_{2g}$ ground level and ^5E_g excited level at $\sim$10 000 cm^{-1}. The contribution from the excited ^5E_g level is negligible to the magnetic susceptibility and MS properties even at room temperature. Due to the spin-orbit coupling interaction and a distortion from O_h symmetry as is the case in enstatite, the ground $^5T_{2g}$ level is completely mixed and splits into 9 levels for D_{4h} symmetry present at the $M1$ site and into 15 levels for C_{2v} symmetry at the $M2$ site.[14] The corresponding set of eigenfunctions ψ_n's and eigenvalues E_n's for Fe^{2+} at $M1$ and $M2$ sites produce different electric-field gradient (EFG) tensors at the nuclear positions, resulting in the characteristic ΔE_Q vs T curves for Fe^{2+} at the $M1$ and $M2$ sites (Fig. 3).

In the case of an axial D_{4h} distortion at the $M1$ site, we have shown earlier for ilvaite[22,27] that the method of Abragam and Pryce,[28] which uses the structural isomorphism between the $^5T_{2g}$ and ^5P levels, was very useful in calculating the thermal characteristics of $\overline{\chi}$ and ΔE_Q in terms of only a few parameters appearing in the appropriate Hamiltonian,

$$H=\Delta(1-l_z'^2)-\zeta_\parallel(l_z's_z)-\zeta_\perp(l_x's_x+l_y's_y), \qquad (1)$$

where Δ is the splitting between the degenerate orbital levels $|\pm1\rangle$ and the orbital singlet $|0\rangle$ level of the ground state $^5T_{2g}$, caused by the axial D_{4h} field. Conventionally[23] the sign of Δ is considered to be positive when the orbital doublet $|\pm1\rangle$ lies energetically lower than the singlet $|0\rangle$ and negative when the pattern is reversed. $l'(l'=1)$ is the effective orbital angular moments of the $^5T_{2g}$ state, and l_z' is the Z component of l. The X and Y components are, respectively, l_x' and l_y'. Each of these orbital states has fivefold spin degeneracy, and s_x, s_y, and s_z are the X, Y, and Z components of spin angular momentum. Due to the covalency effect, the orbital angular moments l_z', l_x', and l_y' of the ground manifold are expressed as $\kappa_z l_z$, $\kappa_x l_x$, or $\kappa_y l_y$, where κ_z, κ_x, and κ_y are covalency reduction factors.[22] For D_{4h}, $\kappa_z=\kappa_\parallel$ and $\kappa_y=\kappa_x=\kappa_\perp$. For similar reasons the spin-orbit coupling constant $\zeta(-104\pm1\ cm^{-1})$ is reduced to $\zeta_\parallel$ and $\zeta_\perp$. The values of κ's and ζ's are determined from data fitting.

In the case of Fe^{2+} at the $M2$ site where the LF has C_{2v} symmetry, we assumed $\zeta_x\approx\zeta_y$ to keep the number of parameters to a minimum for a meaningful interpretation of the experimental results and also because the bond distances do

not differ much in the X and Y directions.[16] Furthermore, we assumed the magnetic molecular X, Y, and Z axes to coincide with the optic axes identified by the optical examination.[12,14] For the distortion due to the orthorhombic C_{2v} symmetry, $|+1\rangle$ and $|-1\rangle$ states are no longer degenerate. Hence we defined the separation between $|+1\rangle$ and $|0\rangle$ states as Δ and the separation between $|+1\rangle$ and $|-1\rangle$ states as $\Delta 1$. The matrices corresponding to $m_J=0$, ± 1, ± 2, and ± 3 were solved as in the case of D_{4h} symmetry to obtain the 15 singlet energy levels and their corresponding eigenfunctions were computed after diagonalization.[22,29]

For deriving the expression for quadrupole splitting for the $3d^6$ electron system, the Hamiltonian representing the quadrupole interaction H_Q was taken from Golding:[23]

$$H_Q=\frac{e^2Q\langle r^{-3}\rangle}{7I(2I-1)}\sum_i\left\{(l_i\cdot I)^2+\frac{1}{2}(l_i\cdot I)-2I(I+1)\right\}, \tag{2}$$

and the resulting average nuclear quadrupole splitting ΔE_Q is

$$\Delta E_Q=3.7[1+(\eta^2/3)]^{1/2}\sum_{n=1}^{15}S_n/D_n, \tag{3}$$

where η is the asymmetry factor, S_n are the matrix elements obtained by perturbing the 15 eigenstates of Fe^{2+} by the quadrupolar Hamiltonian (H_Q), and D_n are the exponential energy values of the above Hamiltonian.[22,23] The value of η was reported to be ~ 0.6 by earlier workers[3,7] for OPX samples.

Using the same eigenvalues and eigenfunctions, expressions for the principal orthorhombic tensor susceptibilities χ_Z, χ_X, or χ_Y (emu/mol/atom) were obtained by using Van Vleck's[30] formula,

$$\chi_J=\frac{g_J^2N\beta^2}{Z}\sum_i\left[(E_i^{(1)})^2/kT-2E_i^{(2)}\right]\exp(-E_i^{(0)}/kT), \tag{4}$$

where $\chi_J=\chi_Z$, χ_X, or χ_Y, and the average susceptibilities $\overline{\chi}=(\chi_Z+\chi_X+\chi_Y,)/3$ for the $M2$ site and $\Delta=(\chi_\parallel+\chi_\perp)/3$ for the $M1$ site, where the D_{4h} and C_{2v} axes were as defined by Goldman and Rossman.[14] Z is the partition function, $E_i^{(0)}$, $E_i^{(1)}$, and $E_i^{(2)}$ are, respectively, the zeroth; first, and second-order perturbed Zeeman energies, N is the Avogadro number, and k is the Boltzmann constant. The above expressions are functions of Δ, $\zeta_\parallel$, and $\zeta_\perp$ in the case of D_{4h} symmetry and of Δ, $\Delta 1$, ζ_x, ζ_y, and ζ_z in the case of C_{2v} symmetry, which were considered as variables during fitting of the experimental results of optical spectra, the thermal variations of ΔE_Q, and the magnetic susceptibilities $\overline{\chi}$, χ_a, χ_b, and χ_c of the OPX samples.

IV. LIGAND-FIELD ANALYSIS

Since the optical levels for Fe^{2+} at the $M2$ site of a bronzite ($x=0.15$) sample are known, we attempted to fit ΔE_Q vs T curves for Fe^{2+} at this site for both samples by substituting $\Delta=2000\,\mathrm{cm}^{-1}$ and $\Delta 1=2350\,\mathrm{cm}^{-1}$ as starting parameters and the isotropic reduction factor ζ to be nearly 90% as reported by Goldman and Rossman,[14] and the ratios Δ/ζ and $\Delta 1/\zeta$ were found to be 21.7 and 27.5, respectively. However, since these parameters could not generate the observed ΔE_Q pattern for Fe^{2+} at the $M2$ site even with a reasonable variation of ζ_i (where $i=x,y,z$), we were forced to vary Δ and $\Delta 1$ in order to fit ΔE_Q and the optical spectra. We tried to maintain the ratios Δ/ζ and $\Delta 1/\zeta$ as close as possible to the starting ratios. During the process of variation of the parameters, it was observed that a change in the sign of Δ and $\Delta 1$ from the above values changed the values of the energy levels, the spectra, and the ΔE_Q vs T curves very significantly. A similar behavior was also found when changing the sign of Δ for the case of axial symmetry.[22,23] The parameters Δ, $\Delta 1$, and ζ_i were varied exhaustively with the help of a computer program to obtain the closest match between the calculated and experimental results.

For the best fitting, we found Δ/ζ and $\Delta 1/\zeta$ to be 20.1 and 34.8 for En_{88} ($x=0.12$) and 21.9 and 35.5 for En_{80} ($x=0.20$). The total splitting of the ${}^5T_{2g}$ level for En_{88} is 3955 cm^{-1} and for En_{80} is 3908 cm^{-1}, and the energy-level patterns are almost identical for both samples. The best-fitted LF parameters, energy-level patterns, and the corresponding eigenfunctions for the $M2$ sites of En_{88} and En_{80} are shown in Tables II(a) and II(b), respectively, and the fitted curves are incorporated with the observed results in Fig. 3. Inspection of the tables shows that ζ_i's are nearly isotropically reduced and the values indicate appreciable overlap between the orbitals of the ligand electrons and those at the Fe^{2+} sites, consistent with the results of the neutron diffraction study.[26] We could also fit the observed ΔE_Q vs T curves for the higher concentrations of Fe^{2+} using the same method (Fig. 3), and the ground splitting was found to be 3754 cm^{-1} for Fs_{87} ($x=0.87$) and 3740 cm^{-1} for Fs_{100} ($x=1$) (to be published).

We noted that the splitting of the ${}^5T_{2g}$ level increases with a decrease of ferrous iron concentration as reported earlier from optical studies,[11–14] in which it was observed that with the increase of Fe^{2+} at the $M2$ site there is a shift in energy of the spectra to longer wavelengths,[11] i.e., to lower-energy values.

The major contributions to ΔE_Q at 400 K are from the lowest and successive excited levels E_{-1}, E_0, E_1, and E''_{-1} and E_2, which were, respectively, 35.8%, 25.1%, 17.8%, 17.7%, and 12.3% for En_{88}. Similarly for En_{80} the corresponding percentages were 35.9%, 25.1%, 17.7%, 17.6%, and 12.2%, respectively. Thus it is seen that there are only small variations for enstatites at the higher-temperature region. However, at 20 K the contributions from the ground level and the first excited level are nearly 99.92% and 0.08%, respectively, for the two samples.

Tables II(a) and II(b) show two groups of excited states, one lying between 2175 and 2221 cm^{-1} and another between 3474 and 3955 cm^{-1} for En_{88}. For En_{80} the corresponding groups lie within 2375–2420 cm^{-1} and 3575–3908 cm^{-1}. Because of relaxation effects and strong vibronic excitations in ferromagnesian silicates, quite broad absorption bands have been observed in the α, β, and γ transitions,[12–14] some

TABLE II. (a) Ligand-field parameters for Fe^{2+} at the $M2$ site ($x=0.12$, En_{88}): $\Delta=1990\ cm^{-1}$, $\Delta 1=3450\ cm^{-1}$, $\zeta_z=-100\ cm^{-1}$, $\zeta_{(x=y)}=-99\ cm^{-1}$, $\kappa_z=0.80$, and $\kappa_{(x=y)}=0.80$. (b) Ligand-field parameters for Fe^{2+} at the $M2$ site ($x=0.20$, En_{80}): $\Delta=2190\ cm^{-1}$, $\Delta 1=3550\ cm^{-1}$, $\zeta_z=-100\ cm^{-1}$, $\zeta_{(x=y)}=-99\ cm^{-1}$, $\kappa_z=0.80$, and $\kappa_{(x=y)}=0.80$.

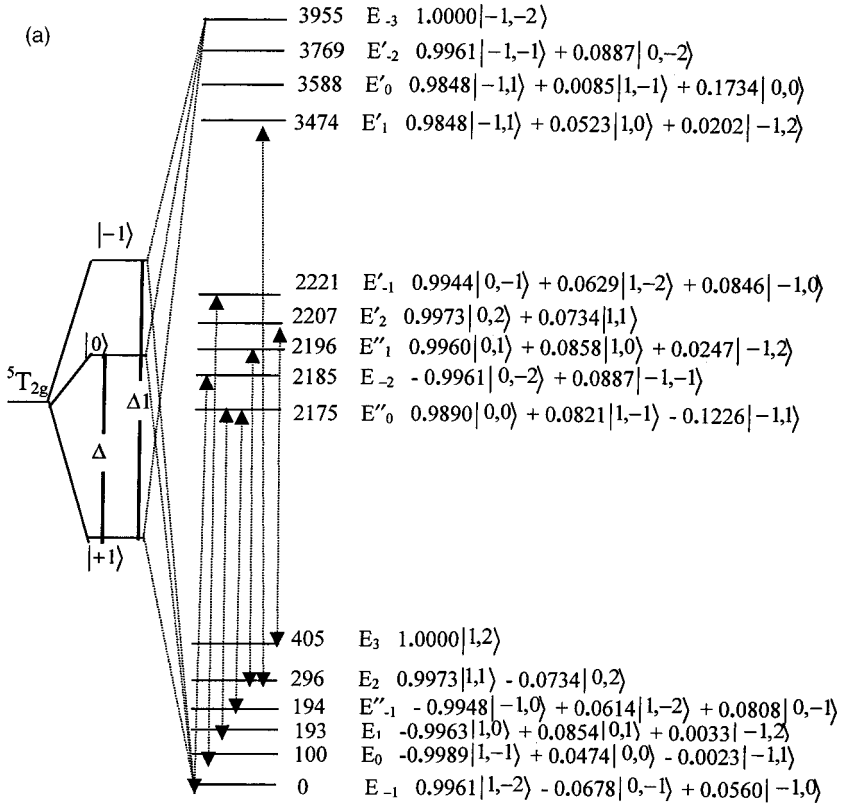

TABLE III. (a) Ligand-field parameters for Fe^{2+} at the $M1$ site ($x=0.12$, En_{88}): $\Delta=-384\ cm^{-1}$, $\zeta_{\|}=-80\ cm^{-1}$, $\zeta_{\perp}=-101\ cm^{-1}$, $\kappa_{\|}=1.00$, and $\kappa_{\perp}=1.00$. (b) Ligand-field parameters for Fe^{2+} at the $M1$ site ($x=0.20$, En_{80}): $\Delta=-417\ cm^{-1}$, $\zeta_{\|}=-69\ cm^{-1}$, $\zeta_{\perp}=-89\ cm^{-1}$, $\kappa_{\|}=1.00$, and $\kappa_{\perp}=1.00$.

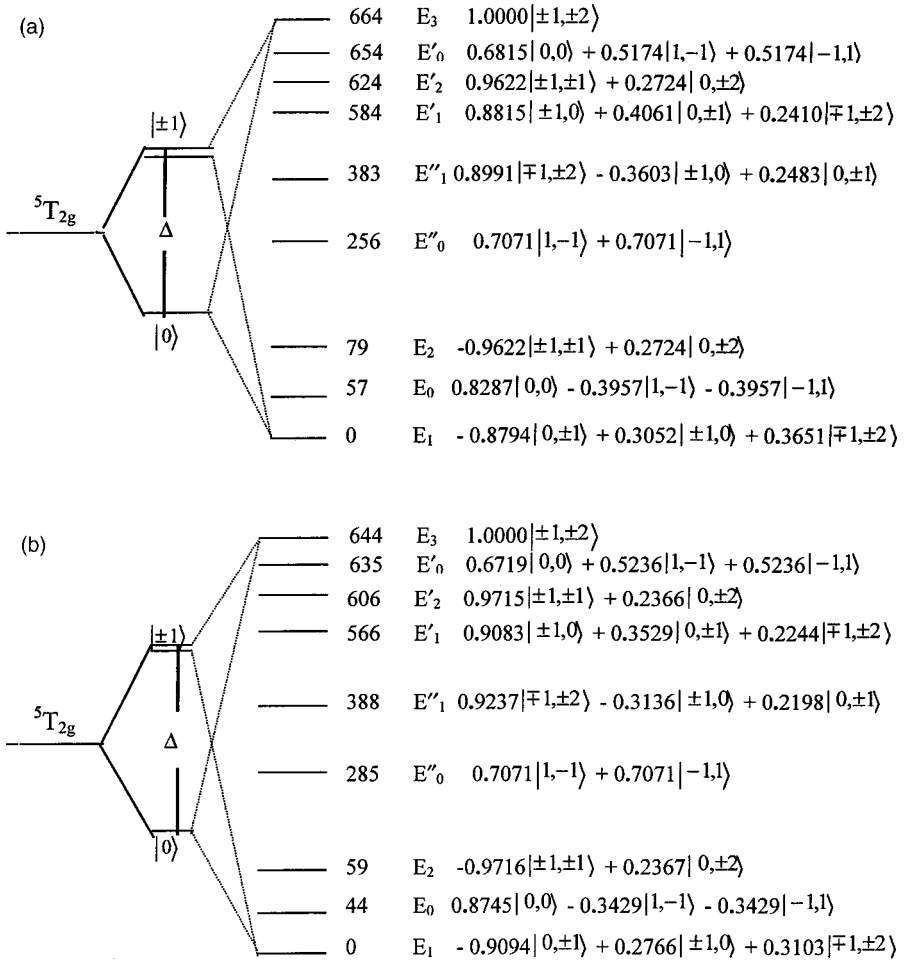

of which were identified with the transitions between the $^5T_{2g}$ components. If we assume the intrasystem transitions[31] to obey the selection rule $\Delta s=0$, $\Delta 1=0$, ±1, we found the prominent transition lines from the ground LF levels to the first excited group of levels to lie between 1802 and 2185 cm^{-1} for En_{88} and between 2000 and 2385 cm^{-1} in the case of En_{80}. Because of strong relaxation effects and thermal excitation, broad absorption maxima are formed containing these lines, like the one observed around 2350 cm^{-1} in a bronzite ($x=0.15$) by Goldman and Rossman.[14] There are also reports of spectral studies[11–13] of enstaties showing sharp absorption peaks appearing between 3100 and 3550 cm^{-1} which were attributed to vibronic excitation of the silicate frame.[14] In the case of En_{88} and En_{80} studied reported here, we found theoretically from Tables II(a) and II(b) that a single prominent transition line from the ground to the second group of excited LF levels is expected at 3474 and 3575 cm^{-1}, respectively. These lines may merge with the vibronic peaks of this region. Thus the present ligand-field analysis explains the observed bronzite spectra, thereby removing the contradiction in the assignments of absorption lines by earlier workers.[11–14]

With the same LF parameters, the thermal characteristics of χ_a, χ_b, and χ_c for Fe^{2+} at the $M2$ site were calculated using the direction cosines between the molecular and crystallographic axes determined from the structural data.[15–17] The average magnetic susceptibility $\overline{\chi}$ is the sum of the contributions from the Fe^{2+} molecular units at $M1$ and $M2$ sites in the same ratio obtained from MS and chemical analyses for En_{88} and En_{80} as given above. The difference between the observed magnetic susceptibility $\overline{\chi}$ and the calculated susceptibility $\overline{\chi}(M2)$ gives the magnetic susceptibility contribution of $\overline{\chi}$ for Fe^{2+} at the $M1$ site.

In the case of Fe^{2+} with D_{4h} symmetry as in the $M1$ site, the thermal characteristics of ΔE_Q vs Δ/ζ curves for various values of ζ/kT have been determined by us[22,27] and others.[21,22] Since ΔE_Q values at different temperatures were known for Fe^{2+} at the $M1$ site for the OPX samples, we obtained a reasonably good estimate of Δ/ζ to lie between 4.5 and 5. To fit the ΔE_Q and the magnetic $\overline{\chi}$ values for Fe^{2+}

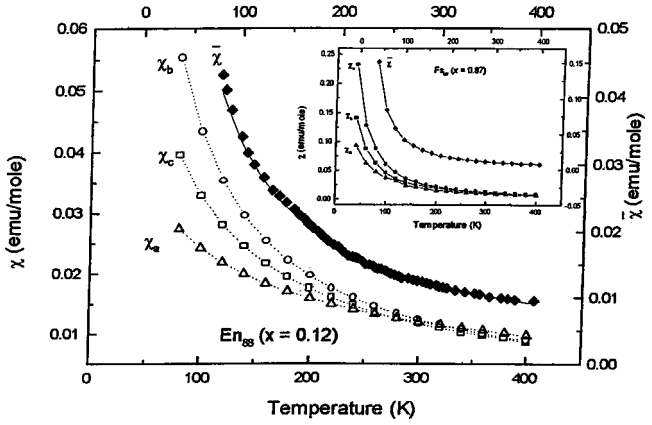

FIG. 4. The thermal characteristics of the average magnetic susceptibility and the directional susceptibilities for En_{88}. The inset shows the magnetic susceptibility for Fs_{87}. Solid circle indicates the experimental data and the lines indicate the LF fitting.

at the $M1$ site simultaneously, we varied Δ and ζ_i ($i=\parallel$ or $\perp$) values, keeping the ratio within the range of values given above. From the best-fitted parameters for Fe^{2+} at the $M1$ site, the ratio of Δ/ζ is found to be 4.3 and 5.3 for En_{88} and En_{80}, which is close to our starting ratio and within the range of values reported for ilvaite[22,27] and for other ferrous iron compounds.[21] The total splitting of the ${}^5T_{2g}$ level is found to be 644 and 664 cm^{-1}, and the excited levels of En_{80} are less separated than those of En_{88}.

The major contributions to ΔE_Q ($M1$) at 400 K is from the ground and first two excited levels, E_1, E_0, and E_2, which are 53.5%, 3.5%, and 54.1% for En_{88} and 52.7%, 3.7%, and 52.6% for En_{80}, respectively. All the other levels contribute negatively to the total splitting. On cooling, the excited levels become depopulated so that their negative contributions decrease and the value of ΔE_Q increases rapidly on cooling. However, at 20 K, the major contribution to ΔE_Q is from the ground level, E_1, being 98.3% and 99.6%, respectively for En_{88} and En_{80}.

Tables III(a) and III(b) show the LF parameters, energy levels, and the corresponding eigenfunctions for Fe^{2+} at the $M1$ site in En_{88} and En_{80} and the fitted MS data are shown in Fig. 3. These tables show that the values of ζ in the parallel and perpendicular directions are anisotropic for D_{4h} symmetry, suggesting a covalency effect. The value of Δ for the D_{4h} is observed to be smaller than the cubic-field splitting as also found in ilvaite[22] and in other ferrous compounds by Ingalls.[21]

The resultant values of the susceptibilities χ_a, χ_b, and χ_c are obtained by adding the contributions from Fe^{2+} atoms at $M1$ and $M2$ sites in the same ratio of occurrence in the two samples. These average susceptibilities ($\bar{\chi}$) are also shown in Fig. 4. The directional susceptibilities from the LF analysis are in the order $\chi_b > \chi_c > \chi_a$, indicating b to be the easy axis, c the intermediate axis, and a the hard axis, as found earlier from single-crystal magnetic susceptibility measurements.[9] These curves show that there is a general agreement of the crystalline susceptibility behavior of enstatites between 400 and 150 K with those of ferrosilite, $FeSiO_3$, reported earlier.[9,10] Magnetic ordering has not been observed by MS studies for Fe^{2+}-diluted silicates[32] and in enstatites with $x < 0.3$ even when studied down to 1.7 K by Shenoy *et al.*[7] However, in the case of the higher Fe^{2+} concentration sample Fs_{87}, magnetic ordering was observed at 26 K.[9] In this case, the usual Heisenberg exchange interaction can be applied on the well-separated ground level using the standard method and χ_a, χ_b, and χ_c characteristics can be simulated (as shown in the inset of Fig. 4) by adjusting the exchange parameter J, where the exchange interaction is given as $\Sigma J = 3k\theta_p/2S(S+1)$, in which the constants have the usual meanings.[18]

As is clear from the above considerations, it was possible to explain quantitatively the different sets of experimental results like the changes in the thermal characteristics of the magnetic susceptibilities and the quadrupole splitting and the blueshift in the optical spectra with the compositional variation in OPX samples by generating the corresponding electronic energy-level patterns using the ligand-field theory. Even in the case of magnetic ordering in the OPX system, the magnetic results can be explained by the same procedure.

Finally, we wish to discuss the physical reasons for the strong site preference of Fe^{2+} over Mg for the distorted octahedral $M2$ site, which has been controversial. Ghose,[16] who originally reported this strong site preference based on a single-crystal x-ray structure refinement of an intermediate orthopyroxene, suggested that the higher degree of covalency of Fe^{2+} at the $M2$ site as evidenced by two short M-O bonds between Fe^{2+} and two underbonded oxygens is the driving force for the strong site preference. The relatively higher degree of covalency for Fe^{2+} at the $M2$ site versus $M1$ has been subsequently confirmed by the difference in the isomer shifts measured by the MS spectra as mentioned earlier. Burns[19] calculated the crystal-field stabilization energy (CFSE)$\approx 1/5(D_Q)$, where D_Q is the cubic field separation of the ${}^5D$ term, for both $M2$ and $M1$ sites in an intermediate OPX to be 11.5 and 11.2 kcal, respectively, and suggested the higher value of the CFSE at the $M2$ site to account for the site preference. It is interesting to note that no such strong site preference has been found in olivine $(Mg, Fe)_2SiO_4$, which also has two different octahedral sites, for which the difference in the CFSE values measured by Burns from optical absorption spectra is greater. To overcome this difficulty, Burns[19] suggested a greater degree of covalency between Fe^{2+} at the $M2$ site and the saturated oxygens bonded to two silicons each in the OPX structure, which is very unlikely. We would like to advance the view that the strong site preference for Fe^{2+} for the $M2$ site originates from the fact that all the degeneracies of the energy levels of the Fe^{2+} ions at the $M2$ site are lifted by the ligand-field effect, resulting in greater stabilization arising from a combination of the site distortion and the relatively greater degree of covalency of the bonds between Fe^{2+} at the $M2$ site and the underbonded oxygens in the orthopyroxene crystal structure.[33–36]

V. CONCLUSIONS

(1) Analysis of the experimental results of magnetic susceptibility and the MS studies reveal that there are small

variations of eigenvalues and eigenfunctions with different Fe^{2+} concentrations in the enstatite region. The ligand-field energy values increase with the dilution of Fe^{2+} in the $M2$ site, which it strongly prefers.

(2) From the LF analysis, directional susceptibilities were found in the order $\chi_b > \chi_c > \chi_a$.

(3) A similar type of LF analysis can be extended to the ferrosilite ($FeSiO_3$) end member of orthopyroxene, considering exchange effect on the LF ground states.

(4) Ligand-field stabilization seems to be the reason for the strong preference of Fe^{2+} for the distorted octahedral $M2$ site in orthopyroxene.

[1] G. M. Bancroft, R. G. Burns, A. G. Maddock, and R. G. J. Strens, Nature (London) **212**, 913 (1966).
[2] G. M. Bancroft, R. G. Burns, and R. A. Howie, Nature (London) **213**, 1221 (1967).
[3] B. J. Evans, S. Ghose, and S. S. Hafner, J. Geol. **75**, 306 (1967).
[4] David Virgo and S. S. Hafner (unpublished).
[5] David Virgo and S. S. Hafner, Am. Mineral. **55**, 201 (1970).
[6] Charles W. Burnham, Yoshikazu Ohashi, S. S. Hafner, and David Virgo, Am. Mineral. **56**, 850 (1971).
[7] G. K. Shenoy, G. M. Kalvius, and S. S. Hafner, J. Appl. Phys. **40**, 1314 (1969).
[8] K. K. P. Srivastava, J. Phys. C **19**, 6407 (1986).
[9] A. Wiedenmann, J. R. Regnard, G. Fillion, and S. S. Hafner, J. Phys. C **19**, 3683 (1986).
[10] S. Ghose, A. W. Hewat, N. Van Dang, and J. R. Weidner, Mater. Sci. Forum **27/28**, 235 (1988).
[11] G. M. Bancroft and R. G. Burns, Am. Mineral. **52**, 1278 (1967).
[12] W. A. Runciman, D. Sengupta, and M. Marshall, Am. Mineral. **58**, 444 (1973).
[13] W. B. White and K. L. Keester, Am. Mineral. **51**, 774 (1966).
[14] D. S. Goldman and G. R. Rossman, Am. Mineral. **62**, 151 (1977).
[15] I. Ito, Z. Kristallogr. **90**, 151 (1935).
[16] S. Ghose, Z. Kristallogr. **122**, 81 (1965).
[17] B. E. Warren and O. I. Modell, Z. Kristallogr. **75**, 1 (1930).
[18] S. Ghose and J. Ganguly, in *Advances in Physical Geochemistry*, edited by S. K. Saxena (Springer-Verlag, New York, 1982), Vols. 2 and 3.
[19] R. G. Burns, *Mineralogical Applications of Crystal Field Theory* (Cambridge University Press, Cambridge, England, 1970).
[20] D. Walsh, G. Donnay, and J. D. H. Donnay, Bull. Soc. Fr. Mineral. Cristallogr. **97**, 170 (1974).
[21] R. Ingalls, Phys. Rev. **133**, A787 (1964).
[22] T. Kundu and D. Ghosh, Phys. Chem. Miner. **17**, 157 (1990).
[23] R. M. Golding, *Applied Wave Mechanics* (Van Nostrand, New York, 1969).
[24] A. T. Rao, Miner. Mag. **42**, 406 (1978).
[25] E. Von Meerwal, Comput. Phys. Commun. **9**, 117 (1975).
[26] B. C. Tofield, *Structure and Bonding* (Springer-Verlag, New York, 1975), Vol. 21.
[27] T. Kundu, Ph.D. thesis, Jadavpur University, Calcutta, 1989.
[28] A. Abragam and M. H. L. Pyrce, Proc. R. Soc. London, Ser. A **206**, 173 (1951).
[29] The complete methodology of the calculation of magnetic susceptibility and the MS can be obtained from the author.
[30] J. H. Van Vleck, *Electric and Magnetic Susceptibilities* (Oxford University Press, London, 1932).
[31] A. S. Chakravarthy, *Introduction to the Magnetic Properties of Solids* (Wiley-Interscience, New York, 1980).
[32] B. Mason B, *Principles of Geochemistry* (Wiley, New York, 1966).
[33] N. Morimoto and K. Koto, Z. Kristallogr. **129**, 65 (1969); S. Ghose, V. Schomaker, and R. K. McMullan, *ibid.* **176**, 159 (1986).
[34] R. O. Sack, Contrib. Mineral. Petrol. **71**, 257 (1980).
[35] R. O. Sack and M. S. Ghiorso, Contrib. Mineral. Petrol. **102**, 41 (1989).
[36] D. Pal, D. Ghosh, and A. K. Pal, Indian J. Phys. **45**, 362 (1971).